Observations of Fast Stochastic Ion Heating by Drift Waves

J. M. McChesney, R. A. Stern,[a] and P. M. Bellan
California Institute of Technology, Pasadena, California 91125
(Received 23 April 1987)

With use of laser-induced fluorescence in the Caltech Encore tokamak, anomalously fast (40× classical) ion heating has been observed and found to correlate with the presence of large-amplitude drift-Alfvén waves. Using numerical simulations we demonstrate that the heating is stochastic and occurs when ion displacement due to polarization drift becomes comparable to the perpendicular wavelength, i.e., when $k_\perp^2\tilde{\phi}/\omega_{ci}B_0 \simeq 1$. Stochastic heating may also be the cause of the anomalously high ion temperatures observed in reverse-field pinches.

PACS numbers: 52.20.Dq, 32.50.+d, 52.35.Kt

We report here observations of fast ion heating (40× classical) in the Encore toroidal device and we show that this heating is due to *stochastic* ion motion in the presence of large-amplitude, current-driven drift-Alfvén waves present in Encore.[1] The ion heating rate was determined with laser-induced fluorescence (LIF).[2] Encore[1] is a small (major radius $R=38.1$ cm, minor radius $a=12.6$ cm) high-repetition-rate (typically 15 shots/s) tokamak. Typical plasma parameters are $Z=1$, $n \simeq (1-2)\times 10^{12}$ cm^{-3}, $T_e \simeq 10-20$ eV, $T_i \simeq 1-10$ eV, $I_p \simeq 1-6$ kA, toroidal field $\simeq 0.01-0.15$ T, shot duration $\simeq 1-5$ ms. The high repetition rate together with excellent plasma reproducibility allows signal-averaging techniques to be employed.

Our measurements represent the first application of LIF to the majority ions of a tokamak plasma. (Previous LIF experiments on toroidal devices were restricted to residual hydrogen neutrals[3] or impurity ions[4] because the majority ions were fully stripped.) In our work singly ionized argon was excited by π-polarized laser radiation at 617.2 nm [transition (1D)$3d\,^2G_{7/2} \rightarrow$ (1D)$4p$-$^2F_{5/2}$]. Ions can either return to the (1D)$3d\,^2G_{7/2}$ state or decay to the (1D)$4s\,^2D_{3/2}$ state emitting a photon at 459.0 nm. The laser system used consisted of a Lambda Physik model FL2001 dye laser using Kiton red dye pumped by a Plasma Kinetics model 451 copper-vapor laser. Typical laser-system parameters were repetition rate 6 kHz, pulse length $\simeq 30$ ns, pulse power $\simeq 20$ kW (at 617 nm). An intracavity Fabry-Perot etalon provided an ultranarrow linewidth of 0.035 cm^{-1}. Scanning the laser across the Doppler-broadened absorption line on a shot-to-shot basis gave the 1D ion-velocity distribution function. Typical Doppler-broadened linewidths of 0.5 cm^{-1} were sufficiently large to render negligible other line-broadening mechanisms (Stark broadening, pressure broadening, etc.). Figure 1 shows the experimental arrangement. Translators allowed nearly the entire torus cross section to be scanned. The target ion density and sensitivity of the light-collection optics gave a spatial resolution of better than 0.1 cm^3. The temporal resolution was set by the laser pulse length of 30 ns. Electron density and temperature were determined with a Langmuir probe[5] biased by a programmable power supply.

Encore plasmas are produced by transformer induction ($E_\phi \simeq 10$ V m^{-1} at breakdown and $E_\phi \simeq 5$ V m^{-1} in the sustaining phase). Figure 2(a) shows LIF-determined ion distribution functions for the first 500 μs of the discharge; Fig. 2(b) shows Gaussian-fitted T_i (normalized to Langmuir-probe[5]-measured T_e) in time. Figure 2 gives an ion heating rate of $\simeq 10^4$ eV s^{-1}. We now show that the most obvious "classical" heating mechanisms cannot account for this fast heating rate.

(i) Direct heating by E_ϕ: The ion and electron drift velocities u_i, u_e due to E_ϕ are determined by $m_i\dot{u}_i = eE_\phi - m_i(u_i-u_e)/\tau_{ie}$ and $m_e\dot{u}_e = -eE_\phi - m_e(u_e-u_i)/\tau_{ei}$ where total momentum conservation gives $m_iu_i + m_eu_e = 0$ and $\tau_{ei}m_i = \tau_{ie}m_e$. The steady-state drift velocities are $u_e = -eE_\phi\tau_{ei}/m_e$ and $u_i = eE_\phi\tau_{ei}/m_i \simeq 1200$ cm s^{-1} with $\tau_{ei} = 3.5\times 10^5 T_e^{3/2}/n\lambda \simeq 1$ μs where $n \simeq 10^{12}$ cm^{-3}, the Spitzer $\lambda \simeq 15$, and $T_e \simeq 12$ eV. Frictional drag of ions on electrons or neutrals will give ion heating

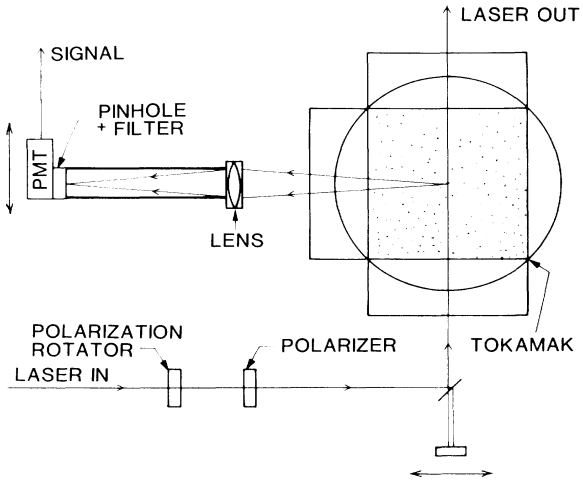

FIG. 1. Experimental setup. The rotator/polarizer combination selects the π polarization.

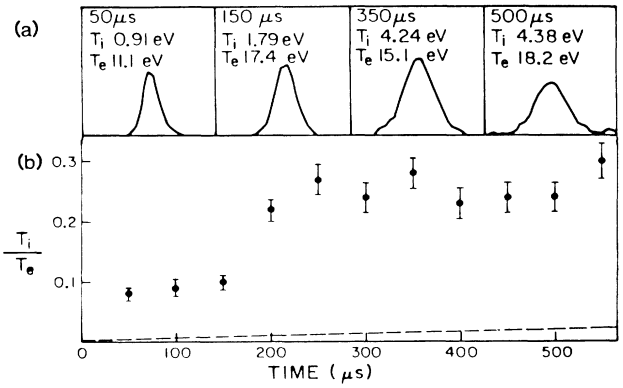

FIG. 2. (a) Ion-velocity distribution functions obtained with LIF. (b) T_i/T_e as a function of time. Dashed line is heating predicted from collisional energy exchange with electrons.

(the ions cannot drag on themselves). The frictional ion heating rate is $dT_i/dt \simeq eE^2\tau_{ei}/m_i \simeq 60$ eV s^{-1}. Similarly, the drag due to neutrals is $(\sigma_{\rm neut} n_{neut} u_i) m_i u_i$ giving

$$dT_i/dt \simeq \sigma_{\rm neut} n_{\rm neut} u_i^3 m_i/e \simeq 4\times 10^{-4}\ \text{eV s}^{-1}$$

with $\sigma_{\rm neut} \simeq 5\times 10^{-15}$ cm^2 and $n_{\rm neut} \simeq 2\times 10^{12}$ cm^{-3}.

(ii) Equilibration with electrons: Electrons heat up to 10–15 eV very rapidly ($dT_e/dt \simeq eE^2\tau_{ei}/m_e \simeq 4.5\times 10^6$ eV s^{-1}) and will then transfer energy to ions at the rate $dT_i/dt \simeq T_e/\tau_{ie}^E$ where the energy equipartition rate is[6] $\tau_{ie}^E \simeq (m_i/3m_e)\tau_{ei} \simeq 35$ ms. Hence this mechanism gives $dT_i/dt \simeq 350$ eV s^{-1}.

(iii) Heating by ion-acoustic or other modes: The only modes observed in Encore were drift-type waves. Ion acoustic waves have not been observed to propagate in Encore (presumably because of the high T_i/T_e ratio) and so can be ruled out.

(iv) Ion Landau damping on drift waves: During the first 50 μs of the discharge, T_i is less than 1 eV so that the parallel ion velocity ($\simeq 1\times 10^5$ cm s^{-1}) is much smaller than the parallel phase velocity of the drift-Alfvén wave ($\simeq 5\times 10^6$ cm s^{-1}) making Landau damping effects negligible.

(v) Heating by drift-wave turbulence: Heating is observed when the drift waves are coherent, i.e., not turbulent.

We propose that large-amplitude drift-Alfvén modes heat the ions stochastically. Earlier plasma simulation studies[7] predicted that low-frequency drift waves could cause significant ion heating, and Hatakeyama *et al.*[8] have observed pronounced ion heating by current-driven collisionless drift waves in a Q machine. Furthermore, Skiff *et al.* have recently observed stochastic ion heating by neutralized ion Bernstein waves.[9]

In Encore the cross-field ion motion due to the drift wave becomes comparable to the drift-wave perpendicular wavelength. Hence, an ion may rapidly traverse regions of widely varying phase of electric potential $\tilde{\phi}$ making its motion stochastic. Consider the motion of an ion in the field of an electrostatic drift wave. In slab geometry ($\theta \to y, r \to x, m/r \to k$, where m is the azimuthal mode number and r is the minor radius), the ion motion is given by

$$m_i\, d\mathbf{v}/dt = q[k\tilde{\phi}\hat{\mathbf{y}}\cos(ky-\omega t) + \mathbf{v}\times B_0\hat{\mathbf{z}}]. \tag{1}$$

When $\omega \ll \omega_{ci}$, Eq. (1) is traditionally solved by use of the guiding-center approximation[10]: $\mathbf{v} = \mathbf{v}_{\rm Larmor} + \mathbf{v}_{E\times B} + \mathbf{v}_{\rm pol}$, i.e., the sum of the Larmor orbital motion, the $\mathbf{E}\times\mathbf{B}$ drift motion, and the polarization drift motion ($\mathbf{v}_{\rm pol} = \dot{\mathbf{E}}/\omega_{ci}B_0$). In this approximation it is assumed that $\dot{\mathbf{v}}_{\rm pol} \ll \dot{\mathbf{v}}_{E\times B}$. However, taking into account the dependence of y on t in the phase of $\mathbf{E}$ gives

$$\mathbf{v}_{\rm pol} = \hat{\mathbf{y}}\frac{\alpha\omega\sin(ky-\omega t)}{k[1+\alpha\sin(ky-\omega t)]}, \tag{2}$$

where

$$\alpha = m_i k^2\tilde{\phi}/qB_0^2. \tag{3}$$

Thus the approximation $\mathbf{v}_{\rm pol} \ll \dot{\mathbf{v}}_{E\times B}$ is incorrect when $\alpha \simeq 1$. This corresponds to the displacement due to polarization drift $\delta y_{\rm pol} = \int v_{\rm pol}\, dt$ becoming comparable to the wavelength, i.e., $k\delta y_{\rm pol} \simeq 1$. When this happens, the guiding-center approximation fails completely, and the particle motion must be calculated exactly. [The fact that the polarization drift is in the direction of $\mathbf{k}$ is a property of electrostatic waves, but not of transverse (e.g., MHD) waves. Thus, only electrostatic waves may be expected to give stochastic heating.]

When we normalize all times to ω_{ci}^{-1} and all lengths to k^{-1}, and define $\nu = \omega/\omega_{ci}$, Eq. (1) becomes

$$\dot{y} + y = \alpha\cos(y-\nu t), \quad \dot{x} = y, \tag{4}$$

where α is given in Eq. (3). Karney[11] has analyzed Eq. (4) in the context of lower hybrid waves where $\nu \gg 1$ and the ions had large initial velocities. In contrast, we consider the case where $\nu < 1$ and the ions start from rest. Two canonical transformations[11] transform (p_x, x), (p_y, y) (where p_x, p_y are canonical momenta) to the action-angle coordinates (I_1, w_1), (I_2, w_2) where $x + p_y = -I_2$, $p_x + \nu t = w_2$, $p_y = (2I_1)^{1/2}\cos w_1$, and $y + p_x = (2I_1)^{1/2} \times \sin w_1$. Three variables describe the state of this system: the Larmor radius $[(2I_1)^{1/2}]$, the Larmor angle (w_1), and the wave phase (w_2). Numerically integrating Eq. (4) gives the ion trajectory in the phase space $((2I_1)^{1/2}, w_1, w_2)$. The threshold for stochastic ion motion is then found by constructing surface-of-section plots. Figure 3 shows a series of surface-of-section plots defined by $w_1 = \pi$ for $\nu = 0.44$ and for increasing α. When $\alpha < 0.7$ most trajectories lie on smooth curves which shows that the ion motion is integrable. For $\alpha \geq 0.8$, however, most orbits are no longer integrable and the ion motion becomes stochastic so that the ions may be heated through the range of velocity space shown. We find similar behavior for ν as low as 0.05.

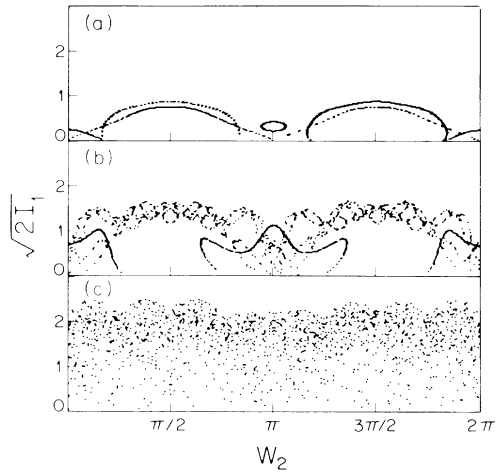

FIG. 3. Series of surface-of-section plots showing the transition to stochastic motion with increasing α for $\nu=0.44$. Each plot shows three different initial positions. (a) $\alpha=0.4$, (b) $\alpha=0.66$, and (c) $\alpha=0.8$.

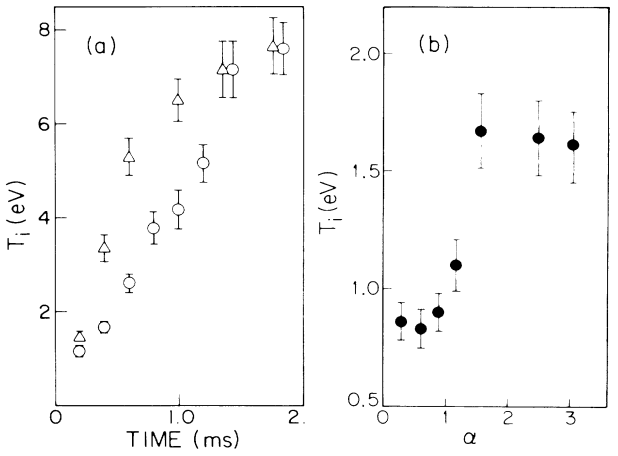

FIG. 4. (a) Ion heating at $r/a=0$ (circles) and $r/a=0.67$ (triangles). $B_0=0.14$ T. (b) Experimental values of peak T_i as a function of α. $B_0=0.03$ T.

[Note that Eq. (4) is integrable for $\nu=0$.] Typically for our experiments $\omega/2\pi\simeq 5$ kHz, $k=m/r\simeq 28.6$ m^{-1} ($m=2$, $r=0.07$ m), $\tilde{\phi}\simeq 5$ V, and $B_0\simeq 0.03$ T giving $\nu\simeq 0.5$ and $\alpha\simeq 1.9$ so that stochastic heating should occur. Experimentally we found that $k_\perp$ increased with B_0 such that α was effectively independent of B_0.

The relative space potential fluctuations of drift instabilities are maximum at the region of maximum density gradient.[1] So if drift-Alfvén waves are responsible for anomalous heating, the highest rates of heating should be expected at the plasma edge. Figure 4(a) shows the time evolution of LIF-determined ion temperature at two positions: $r/a=0$ and $r/a=0.67$. Ion heating rates are clearly higher at the plasma edge. This phenomenon was also observed in Ref. 8. Heating at the plasma center is due to the diffusion of hot ions from the edge. The surface-of-section plots shown in Fig. 3 indicate a distinct threshold for stochastic ion motion (hence ion heating) at $\alpha\simeq 1$. Figure 4(b) shows experimentally determined peak ion temperatures as a function of α. A threshold is evident for $\alpha\simeq 1$–2. α was varied by increasing the amplitude of the $m=2$ drift mode (by increasing the destabilizing plasma current). In the calculation of α, measurements of floating potential, not space potential, were used. In the presence of electron temperature fluctuations these two are not necessarily the same[5]; however, differences between the two are not expected to affect the calculated value of α by more than a factor of 2. The data shown in Fig. 4(a) were obtained with a higher magnetic field than those in Fig. 4(b). The smaller ion Larmor radii obtained with this higher field resulted in more localized ion heating, and higher ultimate T_i before the ions hit the wall. Cross-field diffusion of the heated ions was evidently the main cooling mechanism. Encore plasmas are essentially 100% ionized making ion-neutral collisions and concomitant cooling negligible.

Stochastic ion heating was also directly demonstrated by means of particle simulations. The trajectories of 2000 ions were followed for $\simeq 140$ μs with the representation of the experimentally measured[1] drift-mode electronic potential pattern shown in Fig. 5(a). (Superimposed on this potential pattern is a typical ion trajectory.) The magnetic field was assumed to vary as R^{-1} and motion along the magnetic field was ignored since $k_\perp \gg k_\parallel$. The initial ion positions were randomly distributed across the torus in a normal distribution with a

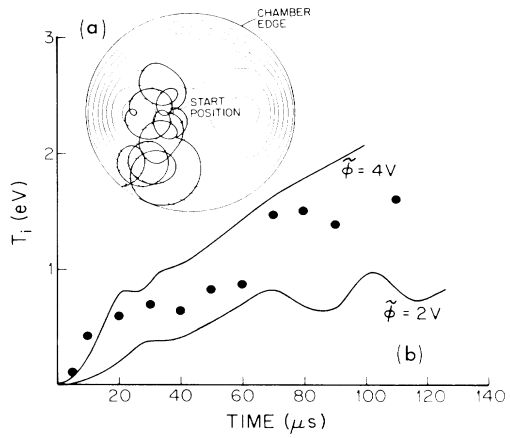

FIG. 5. (a) Contour plot of model drift-wave space potential (contour interval 1 V). This pattern rotates at $\omega_{*d}/2$. Superimposed is a typical ion trajectory. The duration of this trajectory is 625 μs. (b) Comparison of numerical heating results (solid lines) with experimentally observed ion heating due to $m=2$ drift mode.

standard deviation of half the Encore minor radius and the ions were started from rest. Each ion trajectory was integrated and the one-dimensional ion velocity distribution was then calculated every 3.5 μs. Any ions hitting the tokamak wall were assumed lost and were neglected in the calculation of the distribution function. Figure 5(b) compares the results of two simulations ($\tilde{\phi}=2$ V and $\tilde{\phi}=4$ V) to the experimentally observed ion heating. The ion heating rates predicted by these simulations clearly account for the experimentally observed heating rate.

In several respects the Encore plasma is closer to that of a reverse-field pinch (RFP) than that of a tokamak. Like Encore, RFP's have a low magnetic field. They have similar Larmor radii ($\simeq 1$ cm) and the ratio of electron drift speed to electron thermal speed is similar ($u/v_e \simeq 0.1$). Anomalously high ion temperatures and anomalously high rates of ion heating have been observed in all major RFP experiments.[12] Gladd and Krall[13] have shown that drift waves can be strongly destabilized by current in RFP's because of the large value of u/v_e. In RFP's ion heating has been observed[12] to scale strongly with electron drift velocity u suggesting that current-driven modes cause the observed anomalous heating. We showed that α is the critical parameter in determining whether stochastic ion heating will occur. Few $\tilde{\phi}$ measurements have been made on RFP's; however, double-probe measurements made on Zeta[14] showed 50–100-kHz electric-field fluctuations of $(1-3)\times 10^3$ V m^{-1} and perpendicular correlation lengths $\lambda_\perp \simeq 0.05$ m in deuterium discharges with $B \simeq 0.1$ T. These parameters give $\alpha \simeq 1$ so that stochastic heating possibly caused the high T_i observed in Zeta. Both ν and α depend linearly on m_i/Z, and so impurity ions will be stochastically heated faster than H or D ions but may then heat the H or D ions via ion-ion collisions. Also spuriously large values of T_i may be inferred from spectroscopic measurements of the linewidths of heavy impurities.

In summary, we have (i) performed the first LIF experiments on the majority ions of a tokamak, (ii) observed anomalously fast rates of ion heating, and (iii) demonstrated that this heating is caused by stochastic motion in large-amplitude drift-Alfvén waves. Anomalous ion heating in RFP's is possibly due to a similar mechanism.

We thank Mr. F. Cosso for his assistance with electronics. One of us (R.A.S.) would like to thank the Sherman Fairchild Foundation for a fellowship. This work was supported by National Science Foundation Grant No. PHY8312489.

[a]Permanent address: University of Colorado, Boulder, CO 80309.

[1]E. D. Fredrickson and P. M. Bellan, Phys. Fluids **28**, 1866 (1985).

[2]R. M. Measures, J. Appl. Phys. **39**, 5232 (1968); D. Dimock *et al.*, Phys. Fluids **12**, 1730 (1969); R. A. Stern and J. A. Johnson, III, Phys. Rev. Lett. **34**, 1548 (1975); R. A. Stern *et al.*, Phys. Rev. Lett. **37**, 833 (1976).

[3]V. S. Burakov *et al.*, Pis'ma Zh. Eksp. Teor. Fiz. **26**, 547 (1977) [JETP Lett. **26**, 403 (1977)].

[4]C. H. Muller, III, and K. H. Burrell, Phys. Rev. Lett. **47**, 330 (1981).

[5]F. F. Chen, in *Plasma Diagnostic Techniques,* edited by R. H. Huddlestone and S. L. Leonard (Academic, New York, 1964).

[6]B. A. Trubnikov, Rev. Plasma Phys. **1**, 105 (1965).

[7]C. Z. Cheng and H. Okuda, Nucl. Fusion **8**, 587 (1978).

[8]R. Hatakeyama *et al.*, Phys. Fluids **23**, 1774 (1980).

[9]F. Skiff *et al.*, Phys. Rev. Lett. **58**, 1430 (1987).

[10]G. Schmidt, *Physics of High Temperature Plasmas* (Academic, New York, 1979), Chap. 2.

[11]C. F. F. Karney, Phys. Fluids **21**, 1584 (1978).

[12]R. B. Howell and Y. Nagayama, Phys. Fluids **28**, 743 (1985); S. Ortolani *et al.*, Plasma Phys. Controlled Fusion **27**, 69 (1985); H. A. B. Bodin and D. E. Evans, Nucl. Fusion **25**, 1305 (1985).

[13]N. T. Gladd and N. A. Krall, Phys. Fluids **29**, 1483 (1986).

[14]D. C. Robinson and M. G. Rusbridge, Phys. Fluids **14**, 2499 (1971).